

Properties of Amplitude Distributions of Acoustic Emission Signals Generated in Pressure Vessel During Testing

Franciszek WITOS

*Department of Optoelectronics
 Faculty of Electrical Engineering
 Silesian University of Technology*

Krzywoustego 2, 44-100 Gliwice, Poland; e-mail: Franciszek.Witos@polsl.pl

(received October 28, 2018; accepted April 28, 2019)

In the paper, the results of investigations on the properties of acoustic emission signals generated in a tested pressure vessel are presented. The investigations were performed by repeating several times the following procedure: an increase in pressure, maintaining a given pressure level, a further increase in pressure, and then maintaining the pressure at new determined level. During the tests the acoustic emission signals were recorded by the measuring system 8AE-PD with piezoelectric sensors D9241A. The used eight-channel measuring system 8AE-PD enables the monitoring, recording and then basic and advanced analysis of signals.

The results of basic analysis carried out in domain of time and the results of advanced analysis carried out in the discrimination threshold domain of the recorded acoustic emission signals are presented in the paper.

In the framework of the advanced analysis, results are described by the defined by the author descriptors with acronyms ADC, ADP and ADNC. Such description is based on identifying the properties of amplitude distributions of acoustic emission signals by assigning them the level of advancement. It is shown that for signals including continuous AE or single burst AE signals descriptions of such registered signals by means of ADC, ADP and ADNC descriptors and by U_{pp} and U_{rms} descriptors provide identical ordering of registered acoustic emission signals. For complex signals, the description using ADC, ADP and ADNC descriptors based on the analysis of amplitude distributions of recorded signals gives the order of signals with more accurate connection with deformational processes being sources of acoustic emission signals.

Keywords: acoustic emission; multichannel measuring system; amplitude distribution; descriptors; pressure vessel.

1. Introduction

1.1. Descriptors ADC, ADP and ADNC as parameters of acoustic emission signals

An analysis of acoustic emission (AE) signals can be investigated in time, frequency, time-frequency and discrimination threshold domains.

In the framework of the discrimination threshold domain analysis, for each recorded signal, the author defined descriptors of AE signals with acronyms ADC, ADP and ADNC (WITOS, GACEK, 2013; WITOS, 2018a). The calculation of ADC, ADP and ADNC descriptors is performed in a few steps.

- (I) First, the basic AE descriptors are counted at the set values: the discrimination threshold U_d and the duration of the analyzed signal t_s :
 - counts n : number of amplitudes for signal $U(t)$ exceeding the discrimination threshold U_d within time t_s ;
 - count of energy n_E : the number of amplitudes for the square of the signal, i.e. for $U_2(t)$ exceeding the discrimination threshold U_g within time t_s .
- (II) Then the rate of counts above defined descriptors are calculated:

– rate counts N :

$$N = n/t_s, \quad (1)$$

– count of signal power N_P :

$$N_P = n_E/t_s, \quad (2)$$

– rate of normalised count NC :

$$NC = t_n/t_s, \quad (3)$$

where t_n is the sum of time when signal $U(t)$ exceeding the discrimination threshold U_d during time t_s .

- (III) Then the amplitude distributions for these descriptors $N(U_d)$, $NP(U_d)$, $NC(U_d)$ are calculated.
- (IV) Finally, descriptors with acronyms ADC (Amplitude Distribution of Counts), ADP (Amplitude Distribution of Power) and ADNC (Amplitude Distribution of Normalised Counts) are calculated as follows:

- amplitude distributions are made on a logarithmic scale,
- the amplitude distribution is approximated by a fragment of a straight line for the defined range of the discrimination threshold (U_{d1} , U_{d2}): U_{d1} is determined by the minimum of the derivative of amplitude distribution calculated with respect to the discrimination threshold U_g , and U_{d2} is 90% of the maximum value of the recorded signal:

$$y_{ap}(U_d) := \ln(N(U_d))U_d + b, \quad (4)$$

- descriptors are slopes of an approximated straight lines, e.g. for an ADC descriptor:

$$y_{ap}(U_d) := (ADC)U_d + b. \quad (5)$$

Descriptors are not based on values directly measured (amplitudes, AE signal energies). The logarithmic scale for amplitude distributions takes into account the physical characteristics of the studied phenomenon, related to the wave propagation and thickness of the coupling layer. The descriptors take negative values and describe registered AE signals, giving them the so-called level of advancement of AE signal: higher value of descriptor (more flat section of the curve) means higher level of advancement of AE signal.

The level of advancement of the AE signal is related to the level of advancement of the deformational process, the quantitative difference lies in the fact that the deformational process occurs in the area with AE source, and the AE signal is recorded at the measuring point.

Such defined descriptors were successfully applied to work out the classification of the modelled sources of

partial discharges (PD) and PD sources in bars of generator coils (WITOS, GACEK, 2013; WITOS, 2018a). These descriptors calculated for AE signals recorded on the side walls of power transformer tanks are the input data for determination of descriptor maps. In turn, the AE descriptor maps (OLSZEWSKA, WITOS, 2012; WITOS *et al.*, 2011) calculated in a defined frequency band are the basis of the way of location of PD sources in oil power transformers. Such the method of location of PD sources in power transformers has been the patent application (WITOS *et al.*, 2016).

Currently, the author begins to conduct research using the AE method in metals, in particular in storage tanks, pressure tanks and pipelines. In such materials and objects, there are very different deformational processes in which sources generating measurable AE signals are activated (ENNACEUR *et al.*, 2006; MAZAL *et al.*, 2015; MOSTAFAPOUR, DAVOUDI, 2013; QIU *et al.*, 2017; SOKOLKIN *et al.*, 2002). In this paper, the results of assignment of the defined ADC, ADP and ADNC descriptors to the AE signals generated in a pressure vessel are presented. This description has been compared with the description obtained from the analysis of signal properties in the domain of time.

1.2. The measuring system

During investigation, measuring-research system 8AE-PD was used (WITOS *et al.*, 2017; 2019). It is a computer measuring system dedicated to the location and description of PDs in oil power transformers by the acoustic emission method. The architecture of the system, however, allows easy adapting it to measurements of AE signals in other objects than power transformers. In this work, there were investigated AE signals in a pressure vessel. A block diagram of the measuring system is presented in Fig. 1 and the view of measuring system is presented in Fig. 2a.

This system has 8 independent measurement channels. The simultaneous recording of signals in measurement channels up to all 8 channels is possible and it gives the possibility of location of source of AE signals. The gain of the system is fully controlled by software, with the dynamic range of 65 dB for input signal changes (preamplifier + amplifier). The built preamplifier is based on a low noise instrumentation amplifier AD8421 manufactured by the Analog Devices. The amplifier bandwidth is from 20 kHz to 1000 kHz. The system includes the software written in LabVIEW which enables the monitoring of AE signals, their recording in real-time as well as the fundamental and advanced analysis of the recorded signals.

Mounting magnetic holders ensuring stable fixing of the measuring sensor to the tested object are also essential elements of the system 8EA-WNZ. In the presented solution, a set of neodymium magnets together with an appropriate system of springs (Fig. 2c)

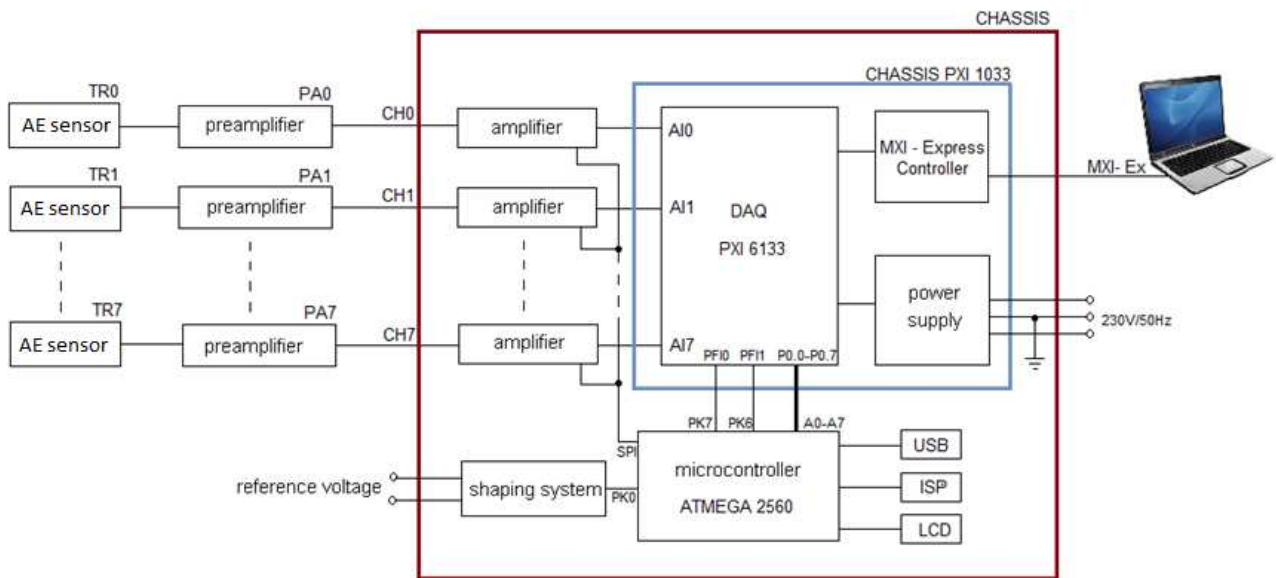


Fig. 1. Block diagram of the measuring system.

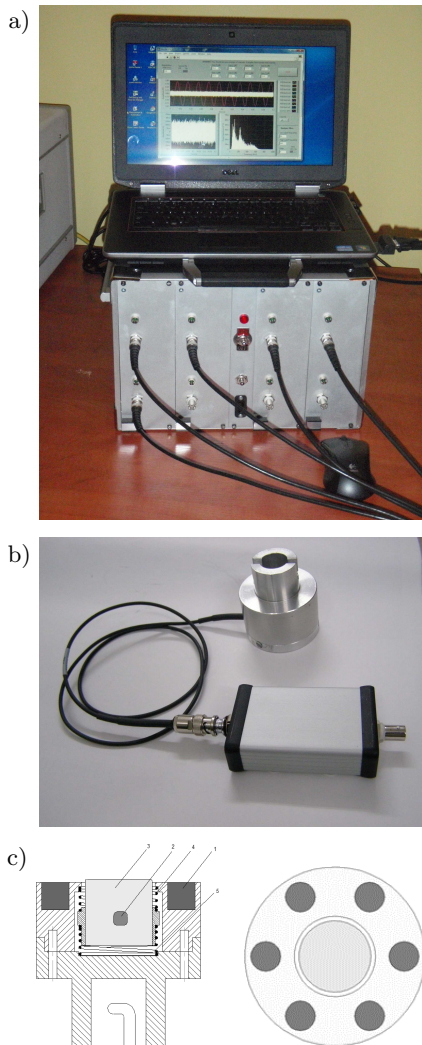


Fig. 2. View of the measuring system 8AE-PD (a), view of the AE sensor in the housing together with the amplifier (b), construction of the magnetic holder (c).

placed in a housing (Fig. 2b) was used. The author have applied to obtain patent protection for this holder (WITOS *et al.*, 2016).

1.3. Testing of the measuring system

In the framework of preparations for investigations of AE signals in pressure vessels, the measuring system 8AE-PD was tested. For this purpose, the investigations of signals generated at various points on the surface of a steel plate with dimensions 970×560 mm and thickness of 4 mm were performed. Figure 3 shows the arrangement of the measuring sensors on the tested steel plate. The system was tested at symmetrical location of the measuring sensors in relation to the signal source of acoustic wave (the source at the point S) as well as at locating the signal source at different distances from individual sensors (the source at the points A, B, C and D). The signals recorded in all the measurement channels for the pulse generated

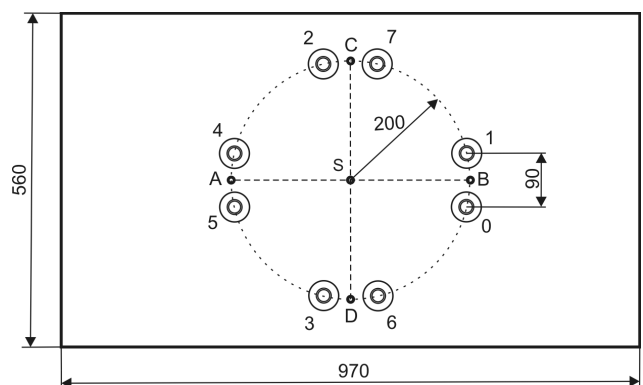


Fig. 3. Arrangement of the measuring sensors on the surface of the tested steel plate together with the marked location of AE sources (A, B, C, D, S).

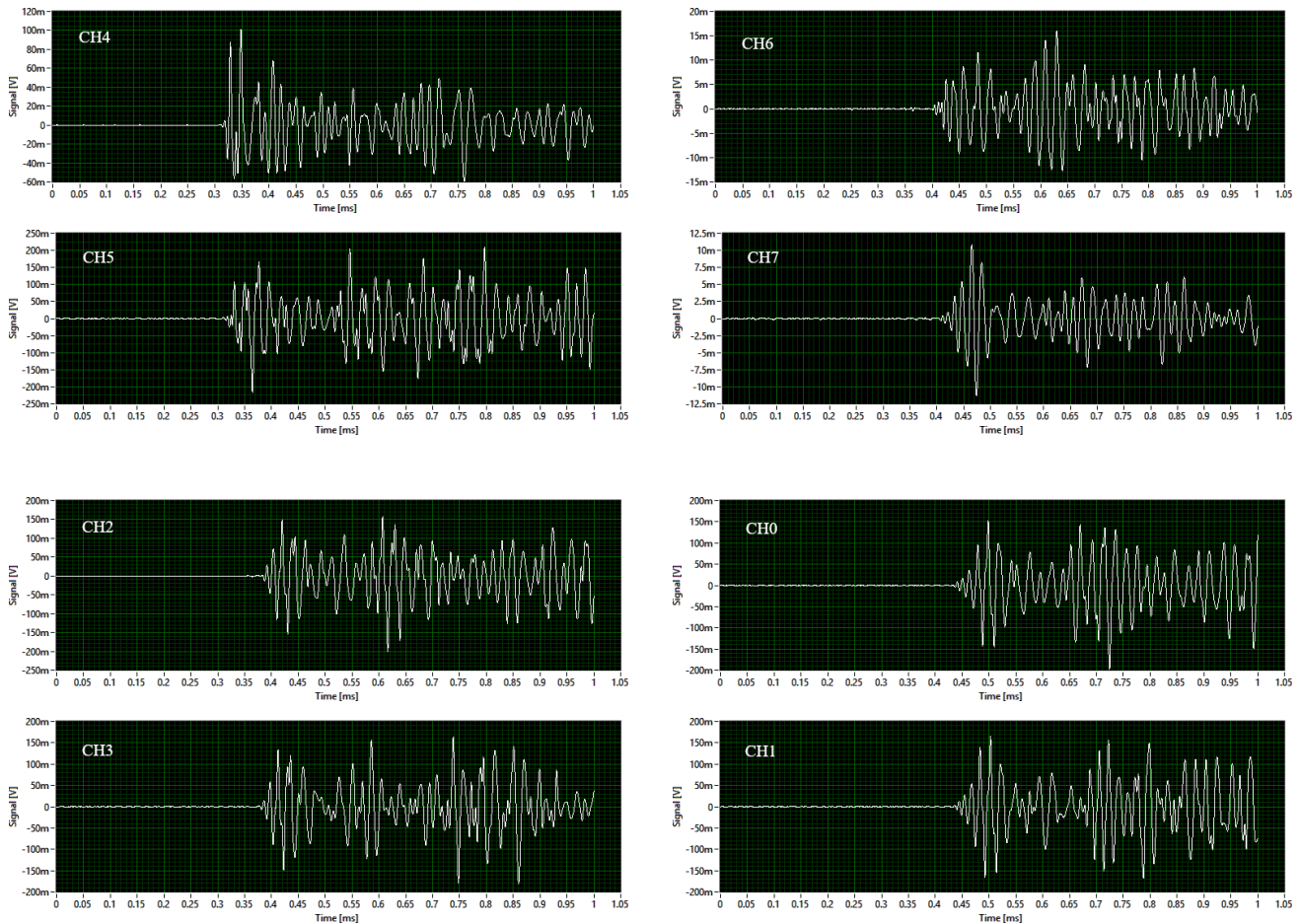


Fig. 4. Signals recorded in the measurement channels CH0–CH7 for the active source in the point A.

at the point A on the tested plate surface are presented in Fig. 4.

The results are grouped in pairs according to the distance from the point A (closest for channels CH4 and CH5, next CH2 and CH3, then CH6 and CH7, and farthest for CH0 and CH1).

As expected, the relative delay times of the recorded signals increase with the increase in distance from the pulse source. Assuming the signal recorded in the channels CH4 and CH5 as a reference signal, it can be stated that the signal in the channels CH2 and CH3 appears with a delay of about 0.08 ms, in the channels CH6 and CH7 with a delay of 0.10 ms and in the channels CH0 and CH1 with a delay of 0.13 ms. The reading of the time differences which occur in reaching the selected AE sensors by the acoustic pulses enables determining the approximate speed of propagation of the acoustic signal in the tested plate. The estimated speed of propagation of the recorded pulses equals to about 3000 ms^{-1} and corresponds to the plate mode A0.

Comparable results were obtained for the measurements made for the acoustic signal source located at the points B, C and D.

The results of the investigations relating to the testing of the constructed research measuring system 8AE-PD confirm the usefulness of this system for studying AE signals as far as the location of signal generation sources is concerned.

2. Investigations of AE signals generated in tested pressure vessel

2.1. The tested object

The object of the study was a compressed-air vessel made of carbon steel (Fig. 5a) with a capacity of 10 m^3 and the allowable pressure $P_a = 27.5 \text{ bar}$. The dimensions of the pressure vessel are given in Table 1. The visual inspection of the outer surface of the pressure vessel showed that layer of protective varnish was in good condition and there were no traces of corrosion.

In the framework of investigations, there were taken measurements of AE signals for two configurations of the measuring sensors on the vessel: P1 and P2. In the paper, there are analysed the AE signals for the arrangement of the sensors in configuration P1 (Fig. 5b).

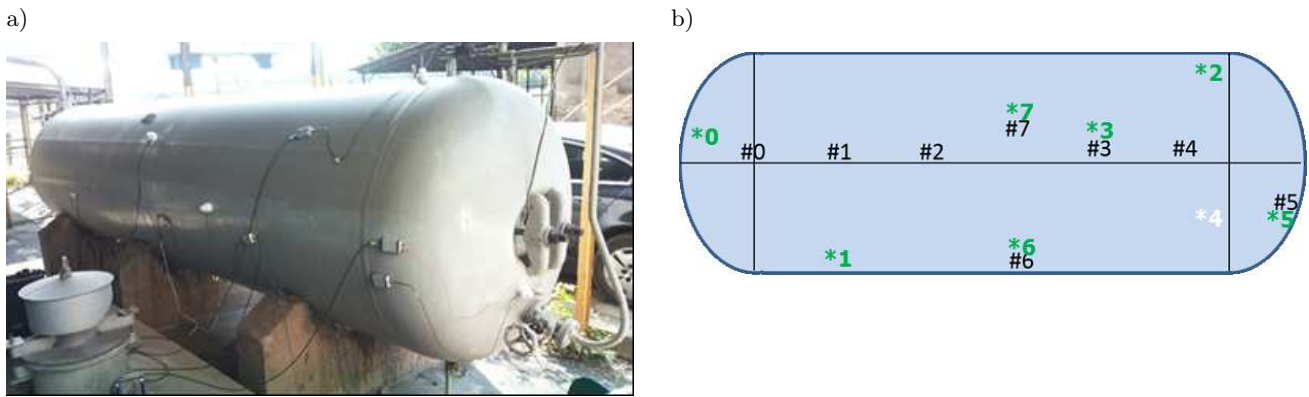


Fig. 5. Tested vessel with AE sensors at P2 configuration and preamplifiers (a), locations of AE sensors on vessel in configurations P1 (#0–#7) and P2 (*0–*7) (b).

Table 1. Dimensions of the tested pressure vessel.

Element	Dimensions [mm]
Coat	thickness × length × width, 23 × 5372 × 2318
Bottom with the manhole	thickness × diameter, 30 × 750
Bottom with the straight-through valve	thickness × diameter, 24 × 750

2.2. Results of the performed investigations

For the tested pressure vessel, the measurements were started from the pressure of the medium equal to 9 bar (33% P_a). Then, the pressure load was increased with the constant speed to the value of 14 bar (50% P_a) and then the constant level of the pressure load was maintained. After that the pressure of the medium was again increased. The procedure was repeated for the pressure loads of 17 bar (61% P_a), 20 bar (72% P_a), 22 bar (80% P_a) and 25 bar (91% P_a).

For the individual constant pressure levels, there were recorded the AE signals (of durations equal to 1 second) in all the eight measurement channels (CH0–CH7). The location of the AE sensors was as presented in Fig. 5b.

The example signals recorded in the measurement channel CH0 for the successive loads of 14 bar, 17 bar, 20 bar, 22 bar and 25 bar are shown within Fig. 6. For the initial loads (14 and 17 bar), the recorded AE signals had the maximum amplitudes at the level of several hundred μV , while for higher pressures the maximum amplitudes reached the values of 2.5 mV.

Moreover, the presented signals give the values which signals have at the input of amplifier within individual measuring channel (Fig. 1). These quantities are obtained in the following way:

- 1) during the measurements, in each measuring channels, the gains are selected so that the values of signals are adapted to the used measuring card (range $\pm 2.5\text{ V}$, 14 bits A/D converter),
- 2) then, the values of signals from the measuring card are divided by the applied voltage gain, giving sig-

nals at the input of amplifier within individual measuring channel (Fig. 6).

Due to such signal processing, the signal analysis results describing the properties of registered signals are independent of the gain used in the measurement system.

The selected 10 ms fragment of the signal from Fig. 6c is shown in Fig. 7. In this fragment one well-located pulse with a peak-to-peak amplitude of $U_{pp} = 4.592\text{ mV}$, several pulses with smaller amplitudes and numerous impulses that are not well located are visible. Many of these numerous pulses have amplitudes with values higher than the noises of the measuring path (noises in the measuring channel A0 are shown in Fig. 6f). These signals were recorded while maintaining a constant pressure in the tank, therefore they describe the dynamic situation and globally these numerous poorly located impulses can be treated as continuous AE.

Summing up, signals recorded during the dynamic maintenance of a constant pressure value in the tested object are the sum of burst AE and continuous AE. The U_{pp} descriptors describe the maximum amplitudes present in the analyzed signal, while the U_{rms} descriptors describe the energy of the analyzed signal. Considering the above, it should be noted that for the signals from Figs 6a–e and 7, U_{pp} descriptors give peak-to-peak amplitudes for pulses with maximum amplitudes, and U_{rms} gives together the energetic properties of the burst AE and continuous AE.

For burst AE, simultaneous recording of signals in a number of measuring channels gives the opportunity to determine the time of reaching a single AE pulse

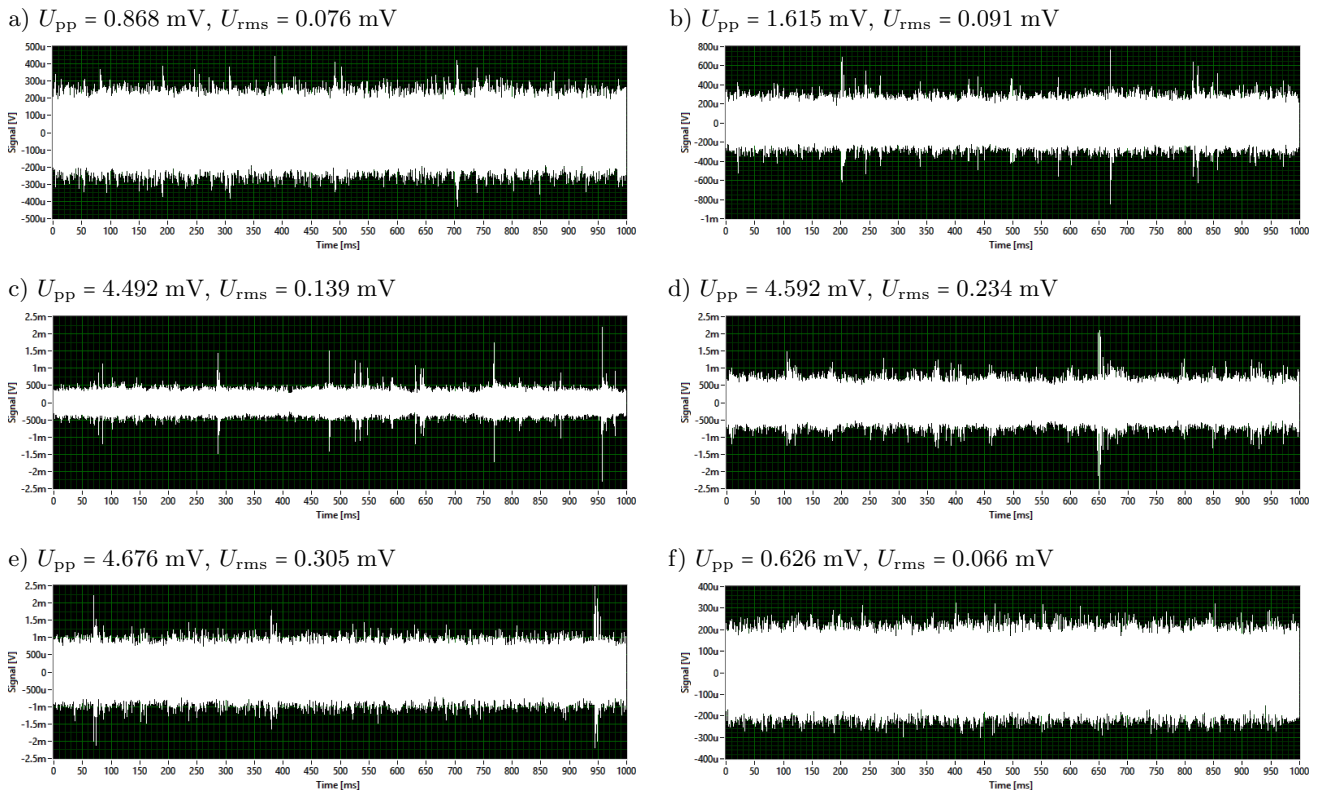


Fig. 6. Example signals recorded in the measurement channel CH0 for various pressures:
 a) 14 bar, b) 17 bar, c) 20 bar, d) 22 bar, e) 25 bar, f) noises.

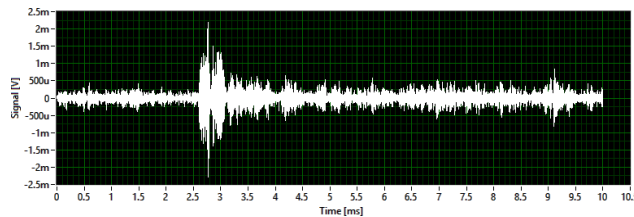


Fig. 7. Fragment of signal with the length of 10 ms being the part of signal from Fig. 6c (positioned in time as 955–965 ms within the recorded signal).

to individual AE sensors and then the location of the source of this signal. An example of a single registered pulse in different measuring channels is shown in Fig. 8.

2.3. Description of registered signals by means of ADC, ADP and ADNC descriptors

A detailed analysis of the properties of recorded signals in the discrimination threshold domain by means of ADC, ADP and ADNC descriptors was started by extracting ten fragments from the signal from Fig. 6c, each with a length of 10 ms. Eight of them contain burst AE signals and two contain continuous AE signals. The descriptors ADC, ADP and ADNC were calculated for such defined signals. The results of the calculations are presented in Table 2 and are ranked by the value of the U_{PP} descriptor describing for these signals. Analysis of these results shows that for each of the

descriptors, the ordering of signals is monotonic, which means that signals having higher values of the time domain descriptors are signals that have higher descriptor values in the discrimination threshold domain, so they are signals with higher level of advancement. The results shown in Table 2 and visualised in Fig. 9 show the similarity of descriptions using the descriptors from time and discrimination threshold domains.

The second stage was describing the whole (i.e. having a length of 1 second) signals recorded during the dynamic maintenance of a constant pressure in the tested object. The results of calculations are presented in Table 3 and visualized in Fig. 10. These results are ranked by the value of the U_{PP} descriptor calculated for these signals. Analysis of these results shows that for descriptors in the domain of discrimination threshold, signal order is still monotone, but U_{RMS} descriptor orders signals in a different way.

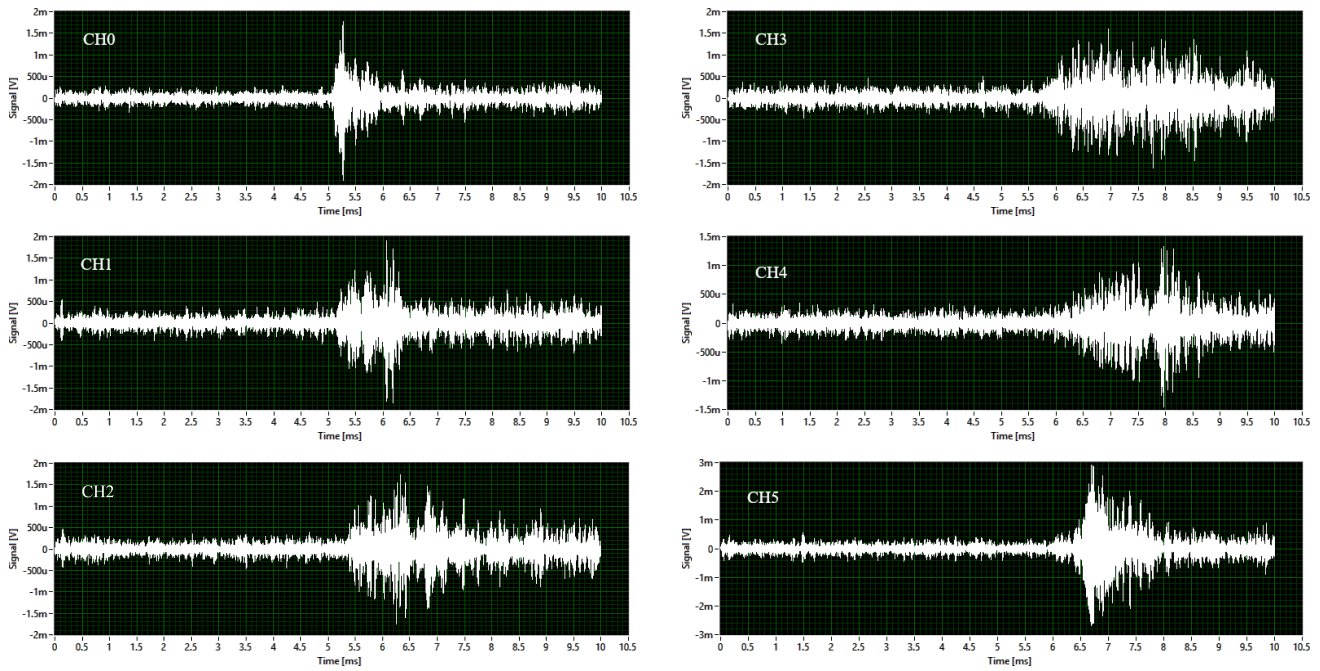


Fig. 8. Fragments of recorded signal at a pressure of 20 bars in measurement channels CH0–CH5 (720–730 ms).

Table 2. Summary of classification of 10 selected signal with the length of 10 ms (selected from signal from Fig. 6c) made by means of descriptors from time and discrimination threshold domains.

No.	Range [ms, ms]	U_{pp} [mV]	U_{rms} [mV]	ADC [a.u.]	ADP [a.u.]	ADNC [a.u.]
1	[955, 965]	4.492	0.237	-1280	-700	-1481
2	[765, 775]	3.449	0.216	-1614	-996	-1960
3	[282, 292]	2.905	0.1945	-2310	-1455	-2604
4	[81, 91]	2.321	0.165	-2952	-1700	-32.44
5	[543, 553]	1.958	0.167	-3203	-1927	-3537
6	[977, 987]	1.856	0.141	-3480	-2027	-3917
7	[808, 818]	1.542	0.158	-4355	-2904	-4579
8	[98, 101]	1.497	0.147	-5116	-3734	-5331
9	[2, 12]	0.841	0.119	-9087	-8186	-7886
10	[407, 417]	0.799	0.126	-9130	-9420	-8771

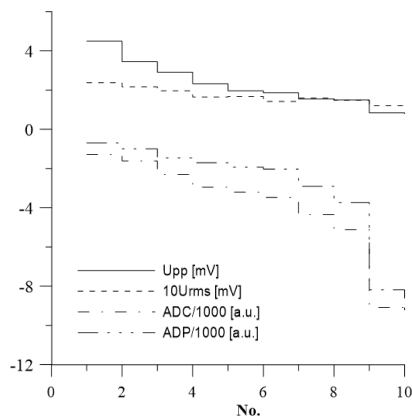


Fig. 9. Visualisation of descriptors from Table 2.

Table 3. Summary of classification of 10 selected signal having the length of 1 second registered during constant pressure of 20 bar made by means of descriptors from time and discrimination threshold domains.

No.	U_{pp} [mV]	U_{rms} [mV]	ADC [a.u.]	ADP [a.u.]	ADNC [a.u.]
1	5.359	0.135	-1596	-810	-1715
2	4.995	0.117	-1722	-895	-1840
3	4.492	0.139	-205	-1317	-2413
4	4.055	0.102	-206	-1121	-2328
5	3.966	0.135	-443	-1379	-2622
6	3.832	0.117	-367	-1350	-2607
7	3.575	0.102	-476	-1328	-2733
8	3.171	0.104	-896	-1623	-3142
9	2.402	0.117	-080	-2551	-4419
10	2.271	0.101	-617	-2851	-4954

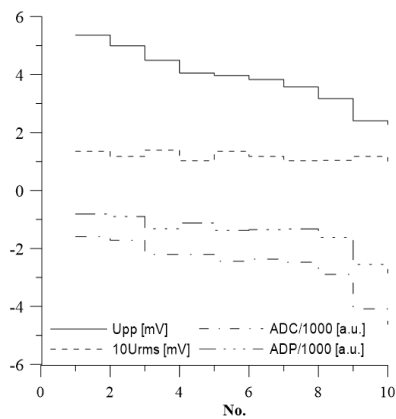


Fig. 10. Visualisation of descriptors from Table 3.

In order to explain the difference in the ordering of whole signals containing signals of both types, i.e. continuous AE and burst AE, obtained at the description by U_{rms} or U_{pp} descriptors, the detailed analysis of the most numerous group of signals registered at 25 bar was carried out. During the tests, such pressure conditions were maintained in the longest time interval of 800 seconds and at that time more than 60 signals were recorded, each one with a length of 1 second. Summary of calculated descriptors for these signals is presented in Figs 11 and 12. In Fig. 11, the signals are ranked by the time of recording signals, while in Fig. 12 they are arranged by the values of the U_{pp} descriptor for signals. There are similarity in the descriptions of U_{pp} , ADC and ADP descriptors, as well as significant differences in descriptions using the U_{rms} and ADP descriptors.

For further analysis, fragments of these signals containing only continuous type AE signals were extracted

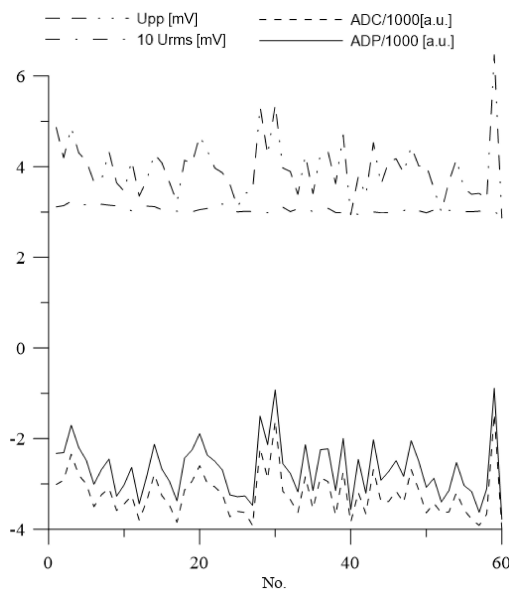


Fig. 11. Descriptors $U_{\text{pp}}(t)$, $10U_{\text{rms}}(t)$, $\text{ADC}/1000(t)$ and $\text{ADP}/1000(t)$ for signals register during constant pressure of 20 bar.

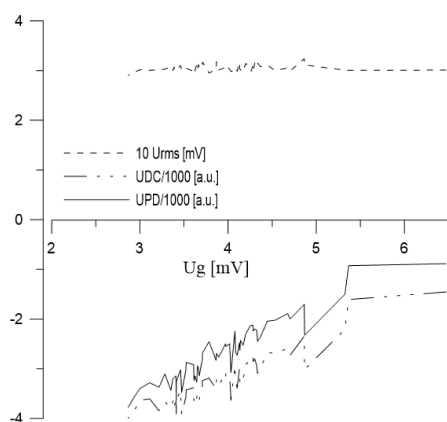


Fig. 12. Descriptors $10U_{\text{rms}}(U_g)$, $\text{ADC}/1000(U_g)$ and for signals register during during constant pressure of 20 bar.

and descriptors were calculated for them. In Table 4 there is a summary of calculated descriptors for such selected signal fragments and for whole signals. The analyzed signals are ordered according to the time of registration counted from the beginning of obtaining the pressure of 25 bar in the tested tank (signal No. 1 was registered at 50 second, and signal No. 6 at 750 second).

Table 4. Summary of descriptions of signals with continuous AE/burst AE type for 6 signals representing 60 signals registered during constant pressure of 25 bar.

No.	Part of signals – only continuous AE			Whole signals – burst and continuous AE		
	U_{rms} [mV]	ADP [a.u.]	U_{pp} [mV]	U_{rms} [mV]	ADP [a.u.]	U_{pp} [mV]
1	0.309	-3241	2.539	0.311	-2326	4.868
2	0.304	-3389	2.569	0.315	-2198	4.303
3	0.300	-3095	2.428	0.312	-2125	4.283
4	0.296	-3311	2.698	0.308	-2134	4.251
5	0.292	-3183	2.532	0.298	-2918	3.609
6	0.293	-3250	2.564	0.304	-2527	4.168

A detailed analysis of the results presented in Table 4 leads to the following conclusions:

- 1) U_{rms} descriptor values for signal fragments containing only continuous type EA decrease with increasing of time (of registering signal from the beginning of obtaining 25 bar in the tested object),
- 2) the U_{rms} descriptor values for the whole signal are slightly greater than the value of the U_{rms} descriptor for the signal fragment containing only the EA of the continuous type,
- 3) the remaining descriptors, i.e. U_{pp} and UDP, do not change monotonically with this time increasing,
- 4) ADP descriptor values for whole signals are much larger than for signal fragments containing only EA of the continuous type.

Figure 13 shows amplitude distributions of power counts $\text{NP}(U_g)$ for the whole signal and for a fragment containing only continuous AE. In this amplitude distribution for the whole signal, there are two contributions: one from continuous AE and the other from burst AE. If we were to separate these contributions, then we would obtain ADP descriptors for such separated phenomena. It is visible, that the ADC descriptor for burst AE is larger than for continuous AE.

In addition, it is worth noting that continuous AE described by U_{rms} descriptors whose value decreases with the increase of time, suggests the relaxing character of this phenomenon. At the same time, the lack of such dependency for the ADP descriptor indicates

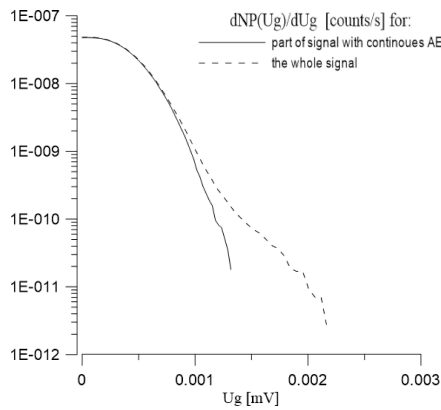


Fig. 13. Amplitude distributions $NP(U_g)$ for signal No. 1 from Table 4.

that level of advancement of registered signals does not change, which means that level of advancement of deformational processes does not change.

The carried out analysis leads to the following conclusions:

- 1) U_{rms} descriptor for registered AE signals during the tests gives only the mathematical value of the power of the recorded signal and does not describe the occurring deformational processes.
- 2) ADP descriptor calculated for all recorded signals describes deformational processes, additionally calculated amplitude distribution $UP(U_g)$ gives the possibility of separating contributions from continuous AE and burst AE.

Description of the properties of signals registered in the CH0 measurement channel while holding in the tested tank constant pressure values during the entire loading process by means ADP and ADC descriptors is depicted in Figs 14 and 15 and Tables 5 and 6.

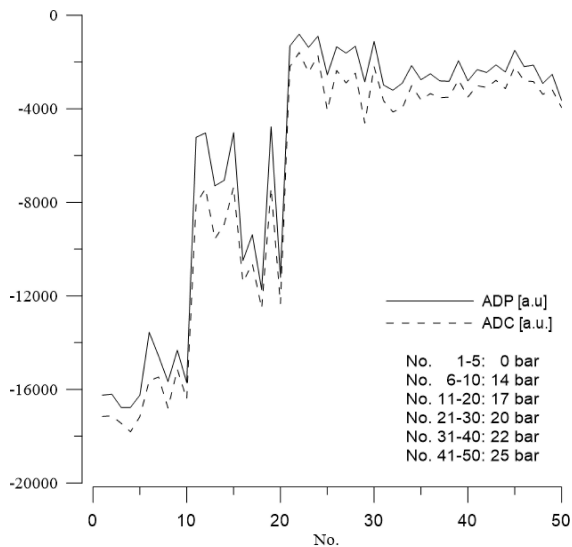


Fig. 14. Descriptors ADC and ADP for signals registered (whole signals) in tested objects during holding constant pressure with different values.

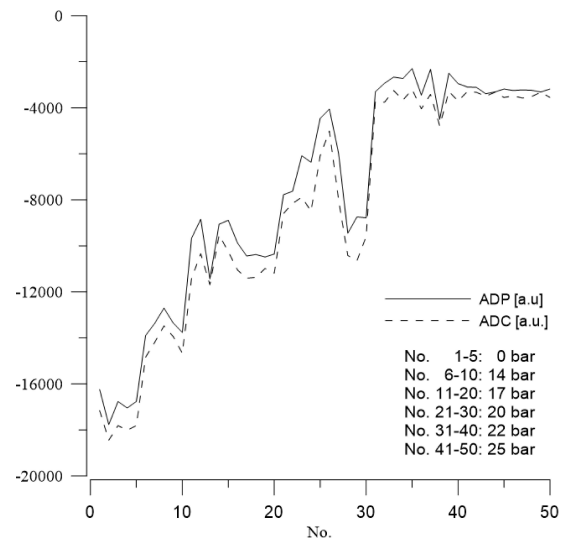


Fig. 15. Descriptors ADC and ADP for part of signals (with continuous AE) registered in tested objects during constant pressure with different values.

Table 5. Average values of ADP and ADC descriptors and their average standard deviations $\sigma(ADP)$ $\sigma(ADC)$ for groups of signals registered while maintaining constant pressure with different values in the examined object. The groups are as in Fig. 14.

Pressure [bar]	ADP [a.u.]	$\sigma(ADP)$ [a.u.]	ADC [a.u.]	$\sigma(ADC)$ [a.u.]
0	-16604	857	-17511	806
14	-14566	1148	-15688	801
17	-7622	2734	-9461	2045
20	-1522	634	-2660	921
22	-2690	364	-3504	383
25	-2425	532	-3039	427

Table 6. Average values of ADP and ADC descriptors and their average standard deviations $\sigma(ADP)$ $\sigma(ADC)$ for groups of signals registered while maintaining constant pressure with different values in the examined object. The groups are as in Fig. 15.

Pressure [bar]	ADP [a.u.]	$\sigma(ADP)$ [a.u.]	ADC [a.u.]	$\sigma(ADC)$ [a.u.]
0	-16917	498	-17847	415
14	-13417	417	-14223	494
17	-942	793	-10923	640
20	-6933	1724	-8142	1696
22	-2965	627	-3685	447
25	-3230	86	-3445	106

Figures 14 and 15 show calculated values of ADP and ADC descriptors for signals recorded during holding in the tested tank constant pressure with different values. Tables 5 and 6 show the calculated average values and their average standard deviations for individual pressure values. Figure 14 and Table 5 describe

the properties of whole signals. Figure 15 and Table 6 describe the properties of signal fragments being continuous AE.

Analysis of average values of ADP and ADC descriptors (for groups of signals registered while maintaining constant pressure with different values in the examined object) for the whole AE signals gives the following description: the signals have a monotonically increasing level of advancement during registration at pressures of 0 (noise), 14, 17 and 20 bar. The level of signal advancement is the highest at a pressure of 20 bar, while during further loading – at pressure values (22 and 25 bar) the level of signal advance is slightly lower than at 20 bar. The biggest fluctuations in the level of signal's advanced occur at a pressure of 17 bar.

Analysis of average values of ADP and ADC descriptors (for groups of signals registered while maintaining constant pressure with different values in the examined object) for fragments of signals being continuous AE gives the following description: the signals have a monotonically increasing level of advancement during registration at pressures of 0 (noise), 14, 17, 20, and 22 bar. Considering the average standard deviations of the descriptors it should be noted that the levels of signal advancement at 22 and 25 bar pressure are similar. For continuous AE, the biggest fluctuations in the level of signal uptake occur at a pressure of 20 bar.

The level of advancement for fragments of continuous AE signals is lower than the level of advancement for whole signals, which means that the deformation processes in which continuous AE and burst AE arise are different processes.

For metal pressure vessels, the main macroscopic sources of AE are:

- a) crack jumps, fracturing and de-bonding of hard inclusions;
- b) plastic deformation development and leakage.

The sources listed as a) generate the burst AE signals, and as b) continuous AE signals.

The most important conclusions resulting from the analysis of recorded signals:

- ADP and ADC descriptors calculated for all recorded signals have maximum values for signals registered at 20 bar pressure and at 22 and 25 bar pressures have lower values;
- values of ADP and ADC descriptors calculated for signal fragments being continuous type EA signals increase monotonically with the increase;
- indicate that, in the entire pressure range used during the tests in the tested object, the initial stages of destruction processes occur with AE source evaluation giving minor AE sources (EN 13554).

3. Conclusions

The results of the performed investigations allow for drawing the following conclusions:

- the measuring system 8AE-PD enables recording AE signals generated during complex changes of the pressure in a pressure vessel;
- U_{pp} and U_{rms} descriptors from time domain give the ordering of the signal with the value of these descriptors;
- ADC, ADP and ADNC from discrimination threshold domain give the ordering of signals with the so-called level of advancements;
- for signals being continuous AE or burst AE with a single signal description of recorded signals by means U_{pp} and U_{rms} descriptors from time domain and ADC, ADP, and ADNC from discrimination threshold domain give the same ordering of signals;
- for complex signals containing both burst AE and continuous AE, U_{rms} descriptors give only the mathematical value of the power of the recorded signals and do not describe the occurring deformational processes;
- for complex signals containing both burst AE and continuous AE, ADP descriptor describes deformation processes, additionally calculated amplitude distribution $UP(U_g)$ gives the possibility of separating contributions from continuous AE and burst AE; different values of descriptors for continuous AE and burst AE show that these signals are generated within different deformational processes.

The performed analyses of the properties of the amplitude distributions confirm the possibility of describing deformational processes in a pressure vessel with the use of the defined ADC and ADP and ADNC descriptors.

References

1. EN 13554:2011:E, *Non-destructive testing – Acoustic emission testing – General principles*.
2. ENNACEUR C., LAKSIMI A., HERVE C., CHERFAOUI M. (2006), *Monitoring crack growth in pressure vessel steels by the acoustic emission technique and the method of potential difference*, International Journal of Pressure Vessels and Piping, **83**, 197–204.
3. MAZAL P., VLASIC F., KOULA V. (2015), *Use of acoustic emission method for identification of fatigue micro-cracks creation*, Procedia Engineering, **133**, 379–388.
4. MOSTAFAPOUR A., DAVOUDI S. (2013), *Analysis of leakage in high pressure pipe using acoustic emission method*, Applied Acoustics, **74**, 335–342.

5. OLSZEWSKA A., WITOS F. (2012), *Location of partial discharge sources and analysis of signals in chosen power oil transformers by means of acoustic emission method*, Acta Physica Polonica A, **122**, 5, 921–926.
6. QIU F., DAI G., ZHANG Y. (2017), *Application of an acoustic emission quantitative method to evaluate oil tank bottom corrosion based on corrosion risk pace*, Insight, **59**, 12, 653–6589.
7. SOKOLKIN A.V., IEVLEV I.YU., CHOLAKH S.O. (2002), *Use of acoustic emission in testing bottoms of welded vertical tanks for oil and oil derivatives*, Russian Journal of Nondestructive Testing, **38**, 1, 902–908.
8. WITOS F. (2018a), *Application of acoustic emission method for partial discharge research in selected elements and devices of electric power systems*, Proceedings of 2018 Joint Conference Acoustics, September, 11–14, 2018, Ustka, Poland, pp. 319–324, IEEE Conference Record: # 44813, doi: 10.1109/ACOUS-TICS.2018.8502315.
9. WITOS F. [Ed.], (2018b), *Investigation of partial discharges in power oil transformers by AE*, LAP LAMBERT Academic Publishing, 94 pages.
10. WITOS F. *et al.* (2017), *Calibration and laboratory testing of computer measuring system 8AE-PD dedicated for analysis of acoustic emission signals generated by partial discharges within oil power transformers*, Archives of Acoustic, **42**, 2, 297–311.
11. WITOS F., GACEK Z. (2013), *Testing of partial discharges and location of their sources in generator coil bars by means of acoustic emission and electric methods*, [in:] *Acoustic emission – research and applications*, W. Sikorski [Ed.], InTech, Rijeka, pp. 117–145.
12. WITOS F., OLSZEWSKA A., SZERSZEŃ G. (2011), *Analysis of properties characteristic for acoustic emission signals recorded on-line in power oil transformers*, Acta Physica Polonica A, **120**, 4, 759–762.
13. WITOS F., OPILSKI Z. (2016), *The method of partial discharges locating, particularly in the power oil transformers, based on the map of acoustic emission descriptors in the frequency domain*, PL Patent: number 223 605, Oct. 2016.
14. WITOS F., OPILSKI Z., SZERSZEN G., SETKIEWICZ M. (2019), *The 8AE-PD computer measurement system for registration and analysis of acoustic emission signals generated by partial discharges in oil power transformer*, Metrology and Measurements Systems, **26**, 2, 403–418.
15. WITOS F., SZERSZEŃ G., SETKIEWICZ M. (2016), *Mounting holder, especially for acoustic emission sensors, to the side surfaces of the transformer tank*, PL Patent, number 223 606, Oct. 2016.